We thank **Referee #1** (L. Maas) for his helpful comments, and appreciate the thoughtful and constructive feedback on the paper, which has helped to improve the manuscript. Appropriate changes will be included in a future version of the revised manuscript, according to detailed responses to each of referee's concerns (below with referee's comments in italic).

Questions raised by referee #1:

1) What profiles for N and U are used to estimate eigenvalue c?

R: The authors acknowledge that inputs used to solve BVP1 were not explicitly presented. These were computed from climatological monthly means in a similar fashion as described in Section 3.1 (i.e. provided from NOAA/OAR/ESRL PSD, Boulder, Colorado and available at http://www.esrl.noaa.gov.). May and October means were computed in appropriate locations along the ISWs seasonal propagation paths – highlighted by green and blue filled circles (for May and October, respectively) in a new version of Fig. 9 (shown below, see panel a). The corresponding vertical profiles for stratification (ρ) and shear (U) are also displayed in new Fig. 9 in additional panels (b) and (c).

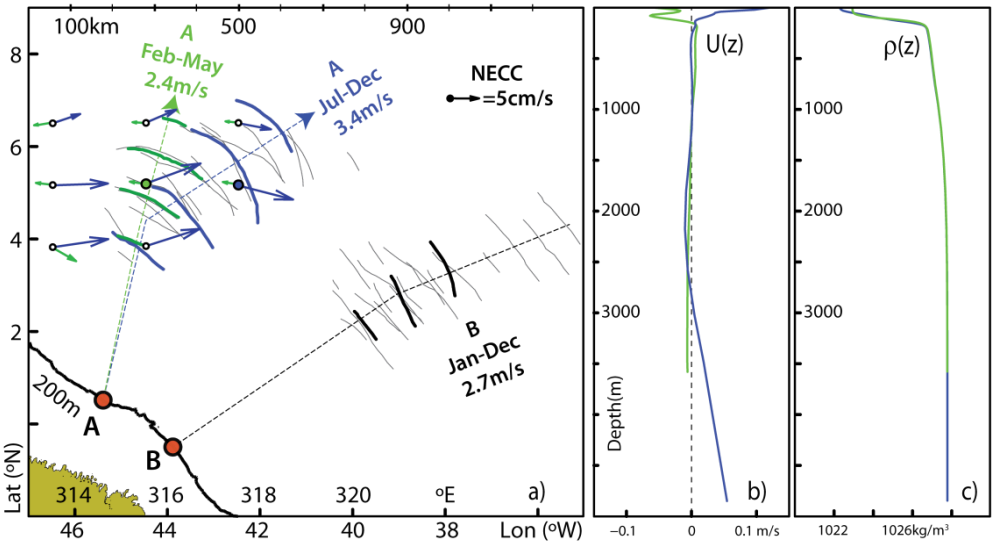

New Figure 9. (a) Same composite map as in Fig. 1 is shown in thin black lines, with two case studies highlighted in thick coloured lines, corresponding to location A and representative of two different seasons: from February to May (in green and dated 27 May 2009) and from July to December (in blue and dated 3 October 2011). Their averaged propagations speeds are also indicated along with idealized propagation paths (in thin dashed lines). Corresponding NECC monthly means (in green and blue for May and October respectively) are shown to depict its seasonal character along the ISWs propagation paths (see also scaled arrow in black). For reference, the case study shown in Fig. 3b is also highlighted in thick black lines, along with its mean propagation speed. (b) Climatological monthly means for horizontal velocity vertical profiles projected along the ISWs idealized propagation path, taken at green and blue filled circles in panel (a) (for May and October, respectively). (c) Same as panel (b) for potential density vertical profiles. See text for more details.

2) *To what extent is the geographical circumstance that the generation area lies in the freshwater (Amazon) outflow region used as a relevant aspect? Is the density gradient below the top layer (N) e.g. stronger than elsewhere, and does this explain the fact that these ISWs have the largest phase speeds ever observed? Or, is this due to an anticipated (yet not clearly substantiated) extra contribution of the NECC?*

R: A direct influence from the Amazon fresh water outflow in the ISW generation and propagation dynamics is not expected to be significant. Typically a NW Amazon plume is observed to develop and extend westward of 47° W (independently of the wind regime, since it is the NBC the leading forcing term), and hence not necessarily related with the ISWs shown in our Fig. 1, which are eastwards of 46° W (see e.g. Figs. 10 and 13 in Nikiema et al., 2007, and references therein).

Another important density front, however, arises as the waves propagate into the NECC, whose influence is of much greater importance. Density gradients along the ISWs propagation paths are indeed strong and are reinforced as the pycnocline vertical extension decreases towards the open ocean (see our Figs. 1, 9 and 11). Nonetheless, density gradients (i.e. *N*) in this region top at around $2x10^{-2}$ s^{-1} (see e.g. our Fig. 11), which are comparable to other regions exhibiting fast propagating ISWs (where *N* at the pycnocline is also of order of 10^{-2}), such as the South China Sea or the Mascarene Ridges (see e.g. Li and Farmer, and da Silva et al., 2015, respectively). Therefore, the authors agree with the referee as he suggests an extra contribution from the NECC to be more likely to explain the elevated phase speeds reported in the manuscript. This is indeed anticipated in the present study using climatological data and SAR evidence, along with other in situ measurements reported in the literature, but as the referee points out a more substantiated approach is needed in order to challenge or confirm this hypothesis. This will be briefly mentioned in the summary as a motivation for further studies including in situ or modelling results.

3) *Can one state something about the other (smaller scale) IWs of O(1 km) wavelength, visible in zoomed versions of the satellite images?*

R: Please see point C below, concerning questions raised by the referee in the main text.

4) *Can one distinguish interfacial from obliquely propagating internal waves?*

R: Despite ISW radar signatures (propagating along the pycnocline) being well established in the literature (see e.g. Alpers, 1985), no successful attempts have yet emerged for the sea surface signatures of internal tidal beams and their impact on the ocean thermocline. An extensive study has also been undertaken in the Bay of Biscay to survey ISWs resulting from the "local generation" mechanism (see New and da Silva, 2002), which also included this same goal, but without any firm conclusions. We recall that satellite borne SARs are able to detect strain rates (i.e. horizontal current gradients) at the sea surface of the order of 10^{-3} s^{-1} (see e.g. Alpers, 1985), which are typical values for short-period internal waves in ocean (which may raise by an order of magnitude for strong nonlinear ISWs). However, while strain rates for IT

beam impacts near the sea surface have never been measured in situ (to the best of our knowledge), model results reveal these to be nearly an order of magnitude smaller and hence unlikely to be imaged in up-to-date SAR imagery. As an example, we present model results from the MITgcm computed for the Mascarene Ridge in the framework of recent investigations by da Silva et al. (2015). These modelling data reproduced quite well the observational SAR ground truth and are therefore considered to yield robust simulations of the surface velocity fields induced by the ISWs and IT beams. Fig. R1 (below) presents in its top panel a model frame for horizontal velocity (*u*, color-coded on the right) in which an IT beam may be seen emanating from the western slopes of an underwater bank (in yellow and reddish colours), and reflecting from the sea surface at around 740 km (between the vertical dashed lines). Farther east a well-developed ISW packet may also be seen propagating rightwards near 760 km. The corresponding surface strain rate associated with these phenomena is depicted in the bottom panel, in which the solitary disturbances may be readily identified (see black arrow) with surface gradients peaking at around 10^{-3} s^{-1}. However, strain rates (which essentially dictate the strength of the radar backscatter) in the vicinities of the beam impact are far less and of the order of the remaining background e.g. beyond 770 km, which are therefore unlikely to be detected in SAR images. Nonetheless, new generation satellite SARs with improved spatial and radiometric resolutions may yield more promising results, which should be explored in the future.

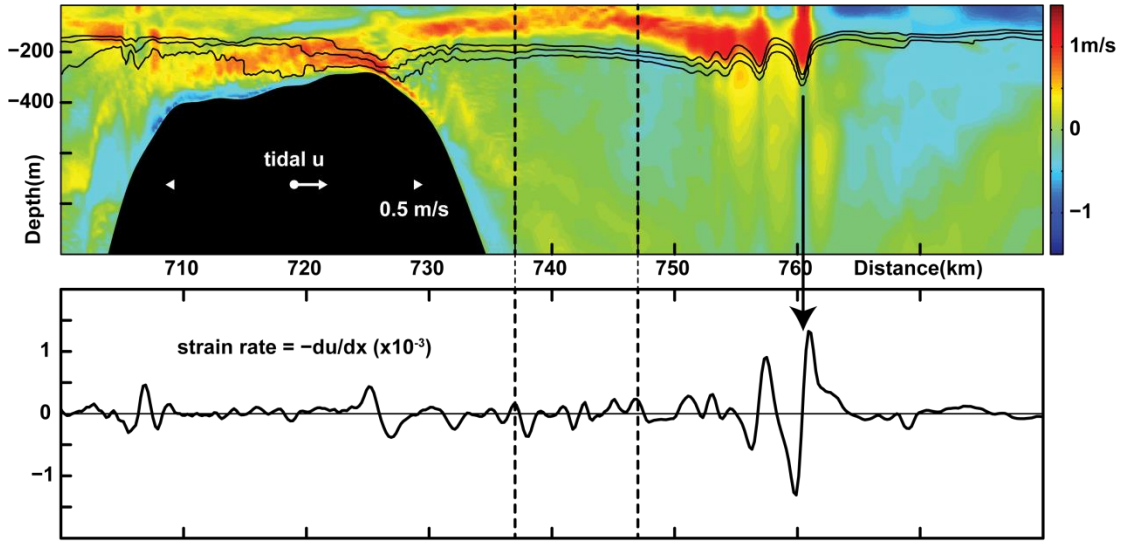

Figure R1. Top panel shows model horizontal velocities (*u*) along with selected isopycnals to highlight the presence of ISWs near 760 km. Bottom panel shows strain rates computed at the surface level (i.e. z=-5m), which yield a proxy of the radar backscatter. Tidal phase is given in white labels in top panel. For reference the region showing the surface reflection of an internal tidal beam is bounded by vertical dashed lines in both panels.

5) *Does 'thermocline shrinking' also explain the increase of the ISW's phase speed and its larger penetration distance?*

R: As predicted, for instance, by the fully nonlinear Dubreil-Jacotin-Long equation (suited for large amplitude ISWs, see e.g. Dunphy et al., 2011), ISWs will indeed become increasingly fast (hence traveling greater distances) with increasingly narrower waveguides – just as suggested by the referee. However, according to Fig. 9, the ISW sea surface manifestations depicted from SAR (taking generation site A for example) are seen north of 3 to 4° N, propagating offshore for

several semidiurnal IT wavelengths, and reaching as far as 7° N. On the other hand, Fig. 11 shows a '*thermocline shrinking*' essentially taking place between 1 and 3 to 4° N, which therefore occurs prior to the ISWs and includes essentially the propagation domain of the IT (i.e. from the shelf-break to 3-4° N) rather than the full propagation range of the ISWs. In fact, these extend farther NE along a pycnocline, whose vertical thickness is fairly constant beyond 4° N (cf. Fig. 11). ISWs from both seasons and emanating from site A are seen extending across the majority of the NECC (in Fig. 1), which is thus more likely to be responsible for the increased phase speeds of the ISWs and penetration distances between July and December (and vice-versa for Feb-May regime).

Questions raised by referee #1 in the main text:
(see also http://www.ocean-sci-discuss.net/12/C1080/2015/osd-12-C1080-2015-supplement.pdf)

A) pp. 2500, line 29. How do we know these are 'low modes'? Typically, the beam size is set by the shelf depth, which, when propagating oceanwards is small (thus of "high mode") compared to ocean depth. Also, the outflow of fresh water suggests generation of interfacial waves on the front (thermocline) separating these waters from the salty deep sea.

R: The particular set of ISW packets addressed in this study, whose inter-packet lengths can be estimated from the SAR imagery, are consistent with semidiurnal interfacial internal tides of the fundamental mode propagating in deep-water (similarly to the Bay of Biscay as discussed in New and da Silva, 2002). Typical horizontal wavelengths are of the order of one hundred kilometres and thus consistent with mode 1 vertical structures computed form BVP 1. Nonetheless, we acknowledge that higher modes may also be generated at the shelf-edge and propagate as internal tide beams into the open ocean. However, these cannot account for the present ISW observations, e.g. in the framework of the 'local generation' mechanism (see e.g. New and Pingree, 1992) as their ray tracing geometry predicts locally generated waves at approximately 100 km from the nearest shelf-break (assuming M_2 frequencies) – and thus in a location much closer to the shelf-break than the SAR observations (see e.g. our Fig. 3). At the same time, generation of large-scale interfacial tides resulting from fresh water outflows (from the Amazon River mouth) and associated density fronts is also unlikely, since these do not account for the waves' semidiurnal period, nor is the river plume extension consistent with the ISW locations (see also point 1 above).

B) pp. 2502, line 15. You mean that the ISW signatures in Fig 1 are a composite of individual trains of ISWs observed? (You could add a number to them and a corresponding number to the lines of Table 1).

R: Fig. 1 is aimed at presenting a composite map resulting from the 17 image acquisitions listed in Table 1. We do not map all the individual waves obtained from all the images, but instead (for clarity) only the strongest ISW signatures were considered and only the leading wave is depicted for each ISW packet (in black solid lines, with a total of 59 packets being represented from the total 17 images). We note that all 17 image acquisitions were made in Wide-Swath mode, each covering 400x400km^2, and hence covering waves generated at multiple tidal cycles

(as many as 5 like in Fig. 3a). Therefore adding a reference number to each of the ISW observations depicted in Fig. 1 would result in an additional 59 labels, ranging from 1 to 17. An attempt to do so was undertaken but soon proved too cumbersome, including in fact several indistinguishable observations.

C) pp. 2503, line 5. Zooming in by 800% on Figs 3a,b, much shorter but often co-aligned IWs (?) are visible, clearly of O (1-2 km) wavelength (definitely shorter than the strong ISW (white bands) of 5-10km according to your estimate). Any explanation? Do they form part of the elusive 'dispersive tail' following (at slower speed) the solitons?

R: We appreciate the referee for highlighting these less evident observations of much shorter-scale ISWs, which were familiar to the authors. In fact, they are a part of the typical ISW field as seen from SAR imagery, frequently appearing alongside their larger mode-1 companions. Several explanations are still being investigated. One possibility includes shorter-scale mode-1 'wave-tails' resulting from mode-2 solitary-like waves traveling deeper down the water-column. Similar observations have been recently documented in independent studies for the South China Sea and in the Mascarene Ridge (see e.g. Guo et al., 2012; and da Silva et al., 2015, respectively). Fig. R2 illustrates this phenomenon in more detail as compared with a typical SAR observation in the Mascarene Ridge. Note that in between the larger mode-1 ISWs, there are other packets (different in nature) separated by approximately half the mode-1 semidiurnal IT wavelengths. A different hypothesis, as the referee points out, includes the sea surface manifestations of dispersive tails originating from the larger ISWs, as discussed for instance in Grimshaw et al. (2014). However, based on the current SAR collection and without further data sources (e.g. in situ or modelling) we can only speculate at this point, and hence prefer to discuss these separate observations as a different subject entirely within forthcoming investigations.

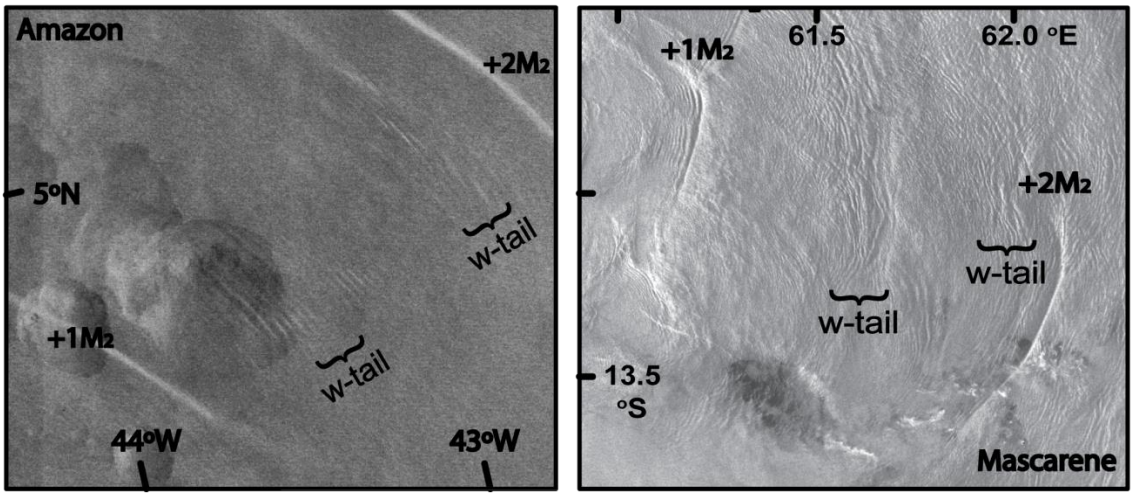

Figure R2. Left panel shows zoomed version of our Fig. 3a, highlighting the presence of shorter-scale 'wave-tails' in between the larger mode-1 ISWs. Right panel shows a subset of an ENVISAT-ASAR image of the Mascarene ridge of the Indian Ocean used in da Silva et al. (2015) and dated March 28, 2009. It shows a typical view of the Mascarene Ridge propagating ISW field. Sea surface signatures of two mode-1 ISW packets and 2 "wave-tails" are delimited within the image subset.

D) pp. 2506, line 11. But the additional 5 cm/s does not at all seem enough to explain the increase in propagation speed from 2.7 to 3.4 m/s... This invites for a deeper wave-current interaction consideration.

R: We agree with the referee since that the additional 5 to 10 cm/s resulting from the NECC climatological means between May and October seem small when comparing the ISW propagation speeds between the same periods (i.e. 2.4 m/s for May and 3.4 in October). However, our goal at this stage of the paper is simply to illustrate that there is in fact a seasonal reverse in the NECC, and that it is in qualitative agreement with both the climatological data and the SAR observations. The next two paragraphs, as the referee suggests are indeed aimed at quantifying how the NECC influences the waves' propagation speeds. This is done in a first approach by means of linear theory and BVP 1, which includes vertical shear, and hence the contribution of the climatological NECC. As discussed in the paper, a reasonable agreement is found for waves in May, but the linear phase speeds using NECC data for October (i.e. 2.5 m/s) yield far less than SAR estimated propagation speeds (around 3.4 m/s). However, we note that measurements performed in situ in November at this same location by Brandt et al. (2002, see their Fig. 1) revealed currents to be much greater than their climatological mean value – between 1 and 1.5 m/s within the ISWs propagation path (see also our Fig. 1). Running BVP 1 including a proxy of these results (instead of the climatological NECC) yields phase speeds between 3 and 3.5m/s), which are in better agreement with SAR estimated propagation speeds. Further studies of wave-current interactions are planned in a near future on the basis of additional high-resolution numerical modelling, as was done for the Mascarene Ridge (see da Silva et al., 2015). See also point (F) below summarizing additional evidence of measured NECC strength (as opposed to its seasonal average).

E) pp. 2506, lines 5 and 8. What profile is measured/assumed here? c seems to be much larger than u. Hence 'resonance' (vanishing of the denominator) is not very likely to occur. Not clear how you obtain this number? You need to specify N(z) (from Fig. 11?) and U(z) before an eigenvalue, c, can be computed.

R: We again agree with the referee since the vertical profiles for stratification and horizontal currents had not been specified in the manuscript. These followed from climatological data (as described in Section 3.1) for May and October in appropriate locations along the ISWs propagation paths, which are now highlighted in a new version of Fig. 9. The corresponding vertical profiles for stratification (ρ) and shear (U) are also displayed in additional panels (b) and (c). As the referee points out, a critical layer (i.e. a layer in which the speed of the background flow matches that of the long linear wave) is unlikely in this case, since linear wave speeds are roughly between 2 and 3 m/s, and the NECC contribution (i.e. U(z)) is at most of the order of 1 m/s.

F) pp. 2507, line 18. Any further info from literature on actual NECC strength (as opposed to its seasonal average)?

R: Complementary results to those reported in Brandt et al. (2002) obtained by drifter observations along the NECC confirm that the climatological data (provided from NOAA/OAR/ESRL PSD, Boulder, Colorado and available at http://www.esrl.noaa.gov) may be underestimated. According to Lumpkin and Garzoli (2005) (see also their Figs. 8 and 9), typical values for April and November not only confirm the NECC reversing character, but also reinforce that corresponding monthly means for near surface currents are of the order of 1 m/s, especially during November.

G) pp. 2508, line 18. Without further explanation, idiosyncratic terminology.

R: Terminologies including solutions 6.1 and 18.5 (i.e. concerning the HYCOM simulations) will be removed from the text, keeping only the corresponding references.

H) pp. 2510, line 13. Explain f and omega.

R: Definitions for 'f' and 'ω' will be included in the final version of the revised text.

I) Table 1. If the range (first line) is 2.25 m, (amplitude 1.12m) how can we distinguish the ascending or descending tide from a measured tidal height of -0.83m? Also: what does it mean that the tidal range varies so much (e.g. 1.34 m at next A, fourth line). This is a function of phase in the fortnightly modulation?

R: An additional column indicating time after high water (TAHW – computed correspondingly for sites A or B) for each image has been added to Table 1 to clarify tidal phases during satellite acquisitions (see also tidal heights and ranges as well as Fig. 2). The referee is correct since images are acquired in different phases of the fortnightly cycle, ranging from neap tides to spring tides (see also Fig. 2). Usually satellite acquisitions are aimed at spring tides, when conditions favour ISW formation (e.g. in the Bay of Biscay or the Mascarene Ridge). However, in the Amazon case ISWs appear to be imaged throughout the entire fortnightly cycle, even despite its strong modulation of the order of 1 m (see our Fig. 2).

J) Figure 11. Seems more representative of different locations.

R: Figure caption will be clarified to make it clear that profile P1 is set just beyond the shelf-break where the pycnocline thickness is still wide and where ITs are being generated, while profile P2 is set just prior to the SAR ISWs observations, where thermocline thickness has already decreased substantially (roughly by 100 m) – and hence belonging to different locations as suggested by the referee.

Additional references (not included in the main text):

Oumarou **Nikiema**, Jean-Luc Devenon, Malika Baklouti, Numerical modeling of the Amazon River plume, Continental Shelf Research, Volume 27, Issue 7, 1 April 2007, Pages 873-899. Doi: 10.1016/j.csr.2006.12.004.

Qiang **Li** and David M. **Farmer**, 2011: The Generation and Evolution of Nonlinear Internal Waves in the Deep Basin of the South China Sea. J. Phys. Oceanogr., 41, 1345–1363. Doi: 10.1175/2011JPO4587.1.

New, A. L., and R. D. **Pingree** (1992), Local generation of internal soliton packets in the central Bay of Biscay, Deep Sea Res., Part A, 39, 1521– 1534. Doi: 10.1016/0198-0149(92)90045-U.

Roger **Grimshaw**, Chuncheng Guo, Karl Helfrich, and Vasiliy Vlasenko, 2014: Combined Effect of Rotation and Topography on Shoaling Oceanic Internal Solitary Waves. J. Phys. Oceanogr., 44, 1116–1132. Doi: 10.1175/JPO-D-13-0194.1.

Rick **Lumpkin**, Silvia L. **Garzoli**, 2005. Near-surface circulation in the Tropical Atlantic Ocean Deep Sea Research Part I: Oceanographic Research Papers, Volume 52, Issue 3, Pages 495-518. Doi: 10.1016/j.dsr.2004.09.001.